Room Temperature Nanojoining of Triangular and Hexagonal Silver Nanodisks

ARTICLE *in* THE JOURNAL OF PHYSICAL CHEMISTRY C · JULY 2013

Impact Factor: 4.77 · DOI: 10.1021/jp403712x

THE JOURNAL OF PHYSICAL CHEMISTRY C

Article

pubs.acs.org/JPCC

Room Temperature Nanojoining of Triangular and Hexagonal Silver Nanodisks

E. Marzbanrad,[†,‡] A. Hu,*[,†,‡] B. Zhao,[†,§] and Y. Zhou[†,‡]

[†]Centre for Advanced Materials Joining, University of Waterloo, Waterloo, Canada

[‡]Department of Mechanical and Mechatronics Engineering, University of Waterloo, Waterloo, Canada

[§]Department of Chemical Engineering, University of Waterloo, Waterloo, Canada

ABSTRACT: Room temperature nanojoining is an important phenomenon that has to be understood well for use in different applications, for example, for assembly of nanoscale building blocks into nanoscale and microscale structures and devices. However, the mechanism for nanoparticle joining at room temperature is not well established. In this research, we employed molecular dynamics simulation to explain how and why silver nanodisks are joined/assembled but with their original shape unchanged. To support our theoretical observations, we compared our simulation results to SEM and HRTEM observations of joined silver nanodisks. It was found that joining at a wide temperature range (1−500 K) can be done through short movement and rearrangement of surface atoms and subsequent elastic or plastic deformation of the particles, resulting in perfect crystal alignment at the joint interface. Our simulation shows the crystal defects such as dislocations due to initial lattice mismatch of the crystals can be sintered out to yield a perfect crystalline structure at the interface between joined particles, which is supported by the experimental observations.

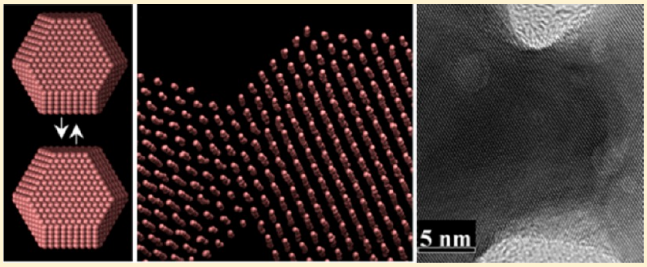

INTRODUCTION

Nanojoining is a challenging but essential step in the nanotechnology for assembly of nanoscale building blocks into 2D or 3D structures.[1] It is well-known that individual atoms may apply attractive or repulsive force on each other depending on their distances, and the atoms in a crystal network will try to find a stable position for themselves in which the net force on each atom becomes zero.[2] Obviously, the most stable configuration of atoms in a crystal is the lowest energy configuration. In this regard, if two particles with clean uncovered surfaces meet each other, they could join to reduce their excess surface energy.[1,3] However, how nanoparticles joined together at low temperature is still unclear. Solid-state bulk and surface diffusion of atoms at a temperature below half of the melting point of bulk material is very slow because there is not enough energy in the system. In sharp contrast, sintering of nanoparticles can occur at a temperature as low as 0.2−0.4 of the melting point.[4−6] Thus, clarification of the nanojoining mechanism is critical in the assembly and joining of nanomaterials.

Nanoparticle self-assembly and joining has been reported in the literature.[7−10] Sun et al. reported that it is possible to transform silver nanospheres to nanobelts through self-assembly of the nanoparticles and subsequent thermal treatment to remove adsorbed surface molecules and sinter the particles.[11] In another research, Tang et al. reported organization of CdTe nanoparticles to nanobelts, in which after partial removal of thioglycolic acid stabilizer layer of the colloidal CdTe nanoparticles by methanol, the CdTe nanoparticles attached to each other and made crystalline CdTe nanobelts.[12] It is interesting that individual CdTe nanoparticles coalesced to become a single crystal. The authors suggested two different mechanisms: one is Oswald ripening, and the other is the direct fusion of the particles for single crystal formation.[11,13,14] However, the mechanism of orientation was not discussed, and a dynamic procedure transferring fused nanoparticles into single crystals was not clarified. Kalsin et al. reported that silver and gold colloidal nanoparticles could join to each other to form a diamond-like lattice structure.[15] They showed that these nanoparticles created unusual binary crystals through electrostatic self-assembly and could join to each other at room temperature to make crystalline particles. Recently, Zhang et al. reported self-assembly of silver nanoparticles at room temperature which led to a 2D array ultrathin film of silver nanoprisms on the glass substrate, providing a tunable plasmon response property.[16] These experimental researches show the importance of nanoparticle joining especially at low temperature.

There are several numerical and theoretical studies on the joining of nanoparticles, but their focus has been in investigation of some unusual behavior of the material at the nanoscale such as melting point of nanomaterials or surface premelting that is used to explain nanoparticle sintering.[17−22] Surface premelting and size-dependent melting behavior in

Received: April 27, 2013
Revised: July 16, 2013
Published: July 22, 2013

nanoscale were usually employed to explain nanoparticle joining. A good example of these theoretical studies is one by Hu et al. concerning low-temperature sintering of silver nanoparticles for flexible electronic packaging.[23] They employed a Monte Carlo simulation to support their experimental results. Size-dependent behavior of the silver nanoparticles was the goal of their model, which was employed to explain low-temperature joining and high-temperature application of the silver nanoparticles as electronic packaging. Detailed results of Monte Carlo simulation of sintering of silver nanoparticles were published by Guo et al.[24] They showed that small silver clusters could join to each other even at 0.01 K. At a higher temperature, attachment and initial joining were followed by sintering of the particles because of the diffusion of atoms. Although Monte Carlo is a simple and powerful method for prediction of the most probable state of a system regarding minimization of the energy of the system, it is not suitable for explanation of the dynamic sintering process. Because, in this method of simulation, the most stable configuration for atoms of the system is found based on a random change in atomic positions and comparing the energy change of the two configurations.[6] On the other hand, the size of the biggest particle in their research was less than 1 nm. Qi et al. show that the cohesive energy of the particles is size dependent.[25] They developed a model to explain cohesive energy of particles as a function of the particle size. Based on their model, cohesive energy of a spherical particle can be calculated using the equation

$$E_p = E_b\left(1 - \frac{d}{D}\right) \tag{1}$$

where E_p is cohesive energy of the spherical particle, E_b is cohesive energy of bulk material, which is equal to 284 kJ/mol for silver,[25] d is equal to atomic diameter, which is equal to 0.288 nm for silver, and D is the diameter of the nanoparticle. Equation 1 shows when the particle diameter becomes around 1 nm or less, the effect of size on cohesive energy of the particle becomes very important. It means changes in total energy of a particle are not linear and extrapolation of the modeling results for subnanometer particles to bigger ones is not accurate. Therefore, another simulation method providing the detailed explanation should be employed to clarify mechanisms of nanoparticles joining.

In this research, we employed a molecular dynamics (MD) simulation method to study room temperature nanoparticles joining. Since silver nanoparticles have attracted intensive research efforts because of their interesting applications, we selected hexagonal and triangular silver nanodisks for MD simulation. The aim of this research was clarification of joining of the particles at a temperature range below half of the melting point of material when there is not surface premelting of the particles. To study the joining mechanism, we perform MD simulation at three different temperatures: 1, 300, and 500 K. 1 K is low enough to deactivate thermally activated mechanisms of joining. 300 K is room temperature, which is our focus, and 500 K is the highest temperature before surface premelting that can affect the joining mechanism. The room temperature joining mechanisms were validated with experimental observations of synthesized, self-assembled, and joined hexagonal and triangular silver nanodisks.

SIMULATION AND EXPERIMENT

a. Molecular Dynamics (MD) Simulation. MD simulation was done with a C++ program developed by the authors, and visualization was done through visual molecular dynamics (VMD) open source software[26] to study room temperature joining of silver nanoparticles. One of the best interatomic potentials for MD simulation of FCC metals is the embedded atom method (EAM potential), developed by Daw and Baskes.[27,28] In EAM, the total energy is defined by eq 2:

$$E_{\text{total}} = \sum_i F(\rho_i) + \frac{1}{2}\sum_{i,j,i\neq j} \phi_{i,j}(r_{ij}) \tag{2}$$

in which ϕ_{ij} is the pair potential between two atoms i and j, which is a function of their distance r_{ij}. $F(\rho_i)$ is the energy required to embed atom i into the electronic gas due to all neighbor atoms which can be calculated by eq 3:

$$\rho_i = \sum_{i\neq j} f(r_{ij}) \tag{3}$$

where $f(r_{ij})$ is the electron density contributed by atom j. The EAM interatomic potential parameters for silver that we used in this research have been calculated by Foiles et al.[29] MD simulations were carried out in the canonical (NVT) ensemble. Temperature was kept constant during simulation according to the Nose–Hoover thermostat.[30] The equations of motion were solved numerically using the Verlet algorithm.[31] Each time step of calculation was 1 fs (1×10^{-15} s). Cutoff radius in this MD simulation was set to 12 Å.

To investigate existence of solid and liquid phases in the system, we used the Lindemann index that was calculated as follows:[32]

$$L_i = \frac{1}{N-1}\sum_{j(j\neq i)} \frac{\sqrt{\langle r_{ij}^2\rangle_T - \langle r_{ij}\rangle_T^2}}{\langle r_{ij}\rangle_T} \tag{4}$$

$$L = \frac{1}{N}\sum_i L_i \tag{5}$$

where L_i and L are the Lindemann index of ith atom and whole particle, respectively, $\langle ...\rangle_T$ denotes the average at temperature T over time, and r_{ij} is the distance between two atoms i and j. As is well-known, Lindeman index equal to 0.1 is a criterion to distinguish solid and liquid phase. If the Lindeman index of an atom or a particle is below 0.1, it is in solid state while the Lindemann index above 0.1 represents high mobility liquid phase.

A hexagonal and a triangular particle were designed, and the MD program was run for each particle for 50 000 time steps to get equilibrium. The hexagonal particle consists of 1785 silver atoms, and the triangle consists of 1288 atoms. In this research, hexagonal nanoparticles were used to show joining in edge-to-side configurations while triangular nanoparticles were used to show joining. Triangular silver nanoparticle in side-to-side configurations was selected for side-to-side joining because of their simple structure at the edges.[33] However, the corner atoms of these particles are not stable because of the sharp angle of the corners of triangle; hence, they are not suitable to show edge to side joining. Therefore, we selected hexagonal silver nanoparticles to observe side to edge joining. In addition, we will report joining of a triangular and a hexagonal particle. To simulate joining in all of the cases, the particles were put far

dx.doi.org/10.1021/jp403712x | J. Phys. Chem. C 2013, 117, 16665–16676

away from each other, which means a distance larger than the cut off radius and the MD program was run for 20 000 time steps before joining. During these 20 000 time steps, two particles reached equilibrium, and initial potential energy of the system could be calculated. After that, the particles were put in close to each other to join freely without any pressure or impact. The distance between nearest points of the particles in this condition must be less than the cutoff radius of the atoms and not too close to push each other away. In this situation, the atoms apply attractive force on each other, the particles become closer and closer, and finally the joining starts. In this research we selected 1 K as the lowest temperature in which thermal energy of the system is very low, and the thermally activated process of joining such as surface or bulk diffusion cannot play a role in joining because the surface and bulk atoms have not enough energy to diffuse. Our focus in this research was room temperature joining, which was modeled at 300 K. Finally, we did simulation at 500 K to investigate role of thermal energy of atoms on the joining.

b. Synthesis and Characterization of Silver Nanoparticles Joining. To synthesize, self-assemble, and join silver nanoparticles, 2.1 g of $AgNO_3$ (Sigma-Aldrich) was added to 60 mL of H_2O and agitated by ultrasonic bath for 1 min to dissolve $AgNO_3$ powder. At the same time in another beaker, 0.68 g of ascorbic acid (Alfa Aesar) and 0.16 mL of poly(methacrylic acid, sodium salt) 40% in water (PMAA) solution (Aldrich Chemistry) were added to 200 mL of H_2O and agitated by an ultrasonic bath for 1 min. Synthesis was started by pouring silver nitrate solution into reducing solution while it was agitating in the ultrasonic bath.

To prepare samples for SEM and TEM observations, 2 min after adding silver nitrate solution to reducing agent, 0.5 mL of this suspension was added to a solution that contained 0.1 mL of PMAA in 3 mL of H_2O. This suspension was agitated in an ultrasonic bath. After 5 min agitation, 0.1 mL of this suspension was added to 3 mL of distilled water. This dilute suspension stirred for 5 min with a magnetic stirrer to wash the surface of the silver nanoparticles from polymer molecules to get better conductivity. 0.02 μL of this dilute suspension was poured on a clean silicon wafer and dried at 70 °C. TEM samples were prepared from the same suspension. One drop of the suspension was poured on a TEM grid, and after drying, the grid was used for TEM observation.

RESULTS AND DISCUSSION

Figure 1 shows the simulation results at 1 K, which was done to check what happened in side-to-side configuration joining of triangular silver nanoparticles when the thermally activated mechanism of sintering such as diffusion was deactivated. Figure 1a shows the triangular nanoparticles just after they were put near each other in a small 3D misalignment (around 5°) before attachment. After first touch at the nearest point of the two particles, they rotated (the left-hand-side particle counterclockwise and the right-hand-side particle clockwise) and aligned as shown in Figures 1b and 1c, respectively. The rotation occurred to make the edges of the particles parallel for a complete contact. Final configuration of the particles after joining is presented in Figures 1c and 1d from two different views. In this simulation, the particles made a joint at the edge, and no more progress was observed. There was a crystallographic orientation between the two particles after joining. As seen in Figure 1d, three (111) planes of the left-hand-side particle were aligned with a few atoms of the right-hand-side

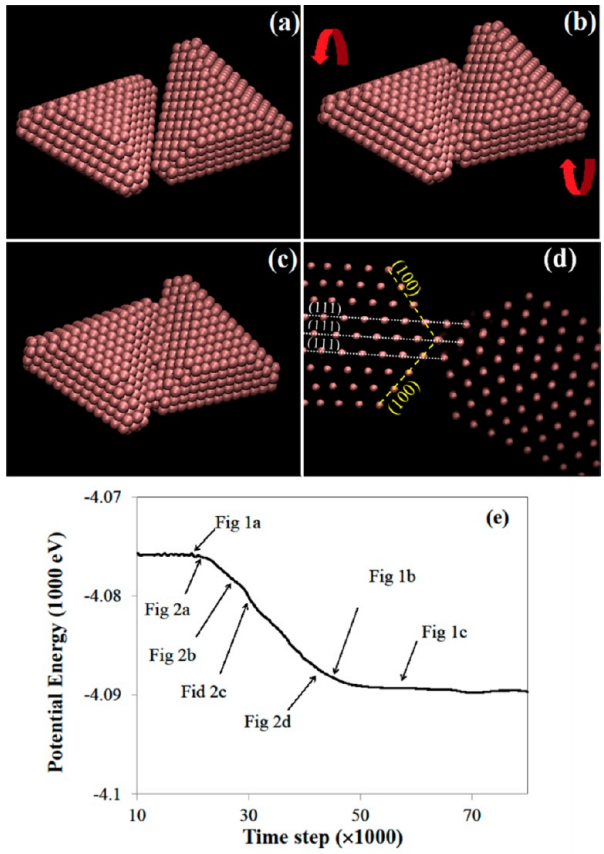

Figure 1. Joining of two triangular nanodisks at 1 K: (a) initial contact; (b) after 45 000 time steps, the arrows show the rotation direction of the particles. (c) Final configuration of the particles, after 57 000 time steps (top view). (d) Structure of interface; the lines show local aligned of atoms at the interface. (e) Potential energy change of the system, corresponding energies of the snapshots of (a–c) and Figure 2a–d are pointed out.

particle. However, the alignment was restricted only to the joint area, and these particles made a line contact. Figure 1e shows the potential energy change of the system during this simulation. The energy of the system corresponding to Figures 1a, 1b, and 1c are marked on this figure. Figure 1e reveals that the potential energy of the system reduced by around 15 eV, which is the driving force for joining of the particles. In Figures 1c and 1d, it is shown that around 30 atoms participated in this joining sequence. The binding energy of silver in fcc crystal is about 2.6 eV for each atom.[34] Therefore, the total energy reduction of the system in the boundary area was around 19.2% of total energy of these atoms if they were in the bulk.

To explain the joining mechanism, a close view of the movement of atoms during joining is presented in Figure 2, and the corresponding energy of each snapshot is marked in Figure 1e. During joining, atoms of the edges of the particles moved to find the most stable position. Figure 2a shows the edge of two particles when they were near each other, before joining. In this image, four atoms were marked to trace their movement during joining. Figure 2b is a snapshot after 8000 time steps. In this figure, the atoms came out of their positions in the right-hand-side crystal and went toward atoms in the left-hand side. Figure 2c is a snapshot after 12 000 time steps showing that the atoms were trying to find their stable positions in the crystal network at the left-hand side. The atoms number one, two, and three

dx.doi.org/10.1021/jp403712x | J. Phys. Chem. C 2013, 117, 16665–16676

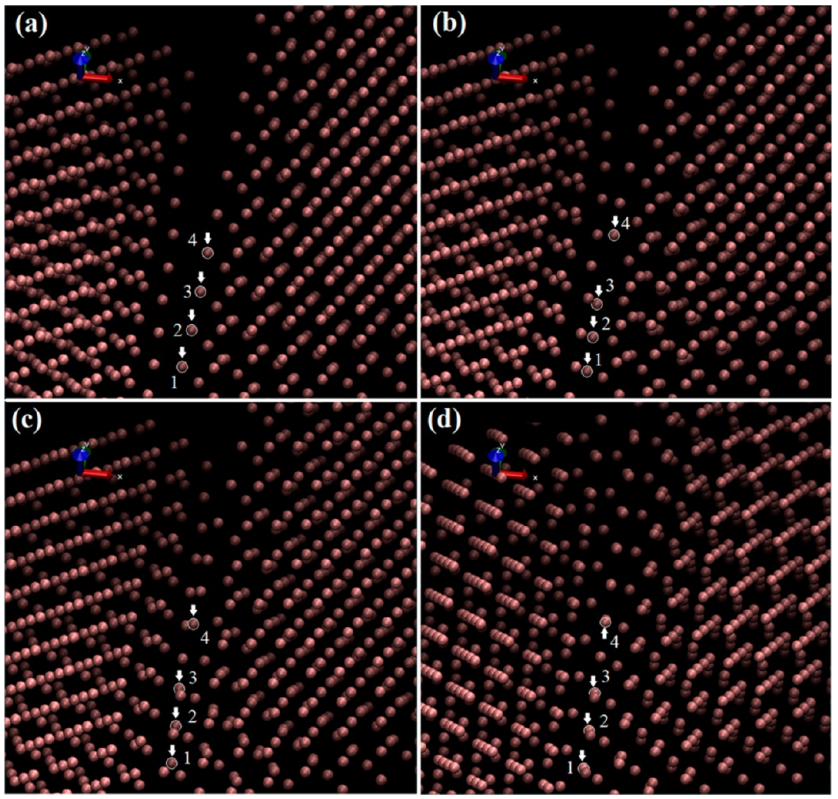

Figure 2. Rearrangement of atoms at the interface between two nanodisks during joining at 1 K: (a) before joining; (b) 8000 time steps after first touch; (c) 12 000 time steps after first touch; (d) final configuration of atoms.

went to the backside of their adjacent atoms from the left-hand-side particle and atom number four went to the front of its neighbors. As mentioned, the atoms migrated to new positions because of the attraction between them and rearranged in a new configuration based on the initial orientation of the particles. Figure 2d shows final configuration of atoms after 27 000 time steps. As seen, the atoms were arranged in new crystal positions and their neighbors in the right-hand side followed the migrated atoms and rearranged themselves. Obviously, movement and rearrangement of atoms were done to decrease the total energy of the system that can be seen in Figure 1e.

Our simulation revealed that even at 1 K, the surface atoms of silver nanoparticles can move and make a contact between two particles because of the attractive forces that exist between the atoms when their distance is less than the cutoff radius of the MD simulation. Since the temperature of this simulation is very low, diffusion is inhibited. Only the joint in line contact is formed by rearranging of surface atoms. This occurs through short movement of the atoms (5−10 Å) under columbic attraction of the adjacent surface atoms of the other particle to reduce the excess energy of surface atoms. Migration of the surface atoms imposes elastic strain that leads to small rotation of the particles. Nanoparticle joining at 1 K as reported here is consistent with previous Monte Carlo simulation results that showed at 0.01 K the silver clusters can join,[24] and further, we provide a clear explanation for the mechanism of joining.

The second simulation was performed at 300 K for the same configuration of triangular silver nanoparticles (Figure 3). Potential energy change of the system during joining is presented in Figure 3a. Similar to the previous case at 1 K, the potential energy of the system reduced through the joining of nanoparticles. However, this curve did not present a simple decreasing curve like the 1 K result (Figure 1e). To elucidate this complex behavior, joining progress has been monitored at different stages. At the beginning, the particles touched each other by attractive forces that existed between them, which led to some reduction in total energy of the system (Figure 3b). After 4000 time steps, nanoparticles completed their initial joining which means the edges of the particles were in a line contact completely (Figure 3c). The joining process was accomplished through a short movement of surface atoms of the right-hand-side particle toward the edge atoms of the left-hand-side particle, the same as what was revealed at 1 K (Figure 2). Similarly, when the atoms at the joint area changed their atomic position and built new aligned structure at the interface, their neighbors in the crystals tended to follow them. This means that the particles were deformed elastically. This elastic deformation induced elastic energy in the nanoparticles. Excess elastic energy of the system, which is shown on the energy curve (Figure 3a) with a circle, was released through first rotation of the particles within the next 10 000 time steps. The direction of rotation of the particles is shown in Figure 3c by a counterclockwise arrow for the left-hand-side particle and a clockwise one for the right-hand-side nanodisk. Configuration of the particles after 38 000 time steps is shown in Figures 3d and 3e from two different views. Looking at the backside of the interface (Figure 3e), it is shown that a gap existed between two particles at the joint area that is marked by an arrow. The surface atoms of the particles in the sides of the gap attracted each other. Therefore, they moved toward each other and filled the gap. During MD simulation from 38 000 to 49 000 time steps, the gap was filled. Figure 3e shows the particles after gap filling. During this process, a little out-of-plane rotation was seen in the particles due to elastic energy release in the system.

dx.doi.org/10.1021/jp403712x | J. Phys. Chem. C 2013, 117, 16665−16676

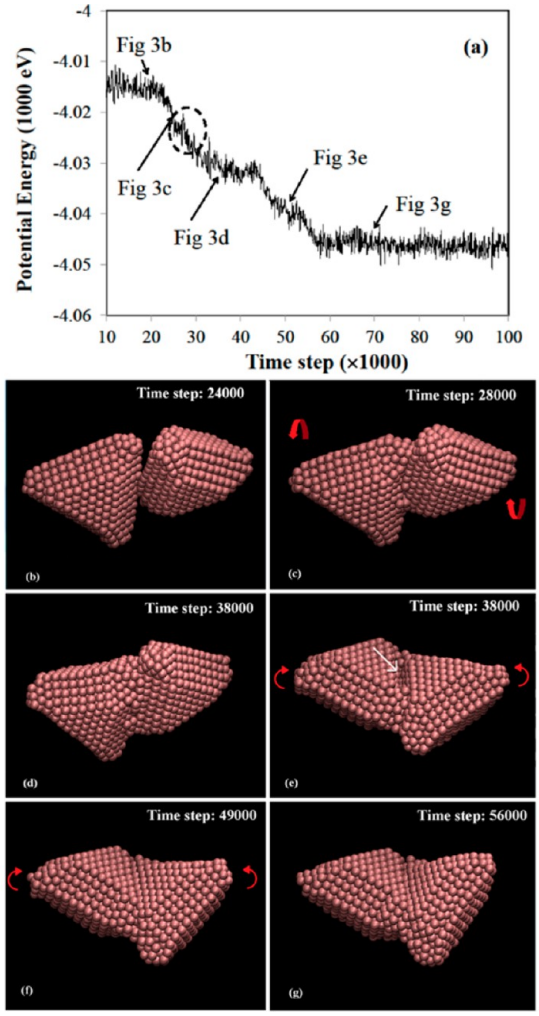

Figure 3. Joining of two triangular nanodisks at 300 K. (a) Potential energy change of the system, corresponding energy of the snapshots of (b)−(g) is pointed out on the graph. (b) First contact of nanodisks. (c) Line contact of nanodisks; the arrows show the rotation direction of the particles. (d) Nanodisks at first step of joining. (e) Gap at the interface; the straight arrow points to the gap between the particles, round arrows show the rotation direction of the particles. (f) Nanodisks after gap filling; the arrows show the rotation direction of the particles. (g) Final configuration of the particles.

Rotation directions of the particles are marked at Figure 3e. The gap-filling process induced additional elastic energy to the system that was released by second rotation of the particles. This energy release is shown in Figure 3a from 49 000 to 56 000 time steps. The arrows in Figure 3f show particles' rotation directions. Figure 3g presents the final configuration of the particles after joining.

To clarify what happens for two nanoparticles after joining from crystal structure point of view, we reduced the size of the atoms in the visualization software to see the crystal structure of the new particle after joining. A cross section of the particles is presented in Figure 4. As shown, the particles were aligned very well during the joining. Dashed lines show twin planes of the triangular nanodisks.[35] As shown in Figure 4, (111) planes on the upper half part of the particles above dashed lines on the Figure 4 were aligned. It is worthwhile to emphasize that there are some irregularities at the bottom of the presented image of the particles in Figure 4. These irregularities come from the

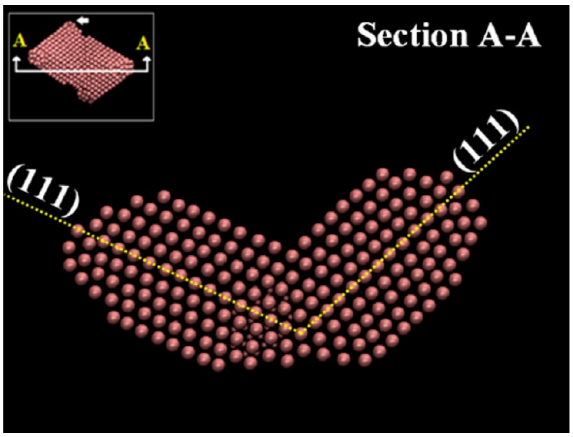

Figure 4. Crystal structure of A−A cross section of two nanodisks after joining at 300 K; (111) planes above dashed lines were aligned.

sharp corners of the triangular particles. The corners' atoms have very high energy and high mobility. Hence, the corners of the particles lost their regularity. For better clarification, this part of the crystal is marked on the added image to Figure 4.

Our MD simulation at 300 K showed an out-of-plane rotation during joining. This rotation was found to be dependent on the geometry of the edge of the particles. The sharp edges of the triangular and hexagonal silver particles can be flattened by increasing the thickness of the particles. In this condition, the edges of the particles have a hcp crystal structure.[33] To investigate effect of flattened edges of the nanodisks on rotation of the particles, we modified the edge of the triangular silver nanoparticles through deleting outer row of atoms from the middle plane of the particles and reran the simulation again. Figure 5a shows the particles before joining at 300 K. Arrows in this figure point to flattened edges of the particles. After joining, these two nanoparticles showed a different configuration (Figure 5b) in comparison to the previous case as shown in Figure 3g; two particles joined to each other without such rotation. Figure 5c shows alignment of (111) planes of the nanodisks at the interface. Comparison between Figures 5c and 4 reveals that in both case [111] directions of the nanodisks aligned at the interface. The presented result in Figure 5 proved that the surface plane of the edge of the particles plays an important role in final configuration of the joined particles while alignment direction of the particles follows the same crystallographic orientation. In other words, rotations were done because the particles wanted to align in a certain crystallographic direction that is [111]. These kinds of rotations during joining of nanoparticles are also reported in other simulations.[24] It is important to mention that this out-of-plane rotation was not observed at 1 K since the particles have not enough energy to extend their interface by rotation.

Not only the structure of the particles at the edges but also their contact direction can affect the joining of the particles. We further investigated the effect of contact direction of the particles on the final configuration and crystal structure of the joint area because of its potential importance in the joining. To do that, we simulated the joining between two hexagonal nano particles at 300 K in edge-to-edge configuration. Figure 6a shows the configuration of the particles in early stage of joining where first contact of the particles took place. Surface atoms of these two silver hexagonal nanoparticles were moved in the

dx.doi.org/10.1021/jp403712x | J. Phys. Chem. C 2013, 117, 16665−16676

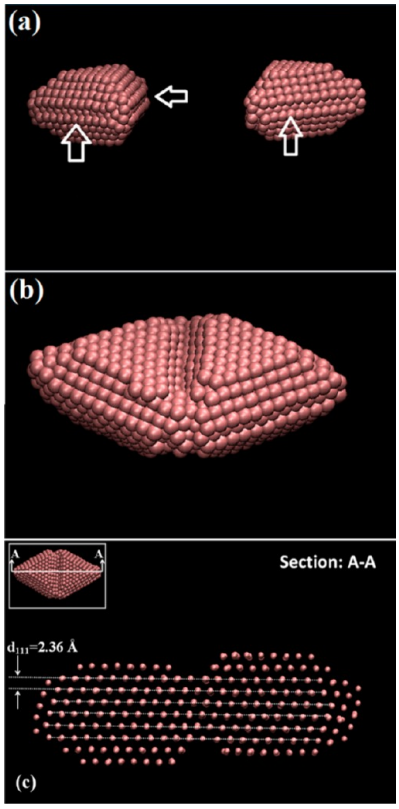

Figure 5. Joining between two flat-edge triangular nanodisks. (a) Before joining, the arrows pointed the flattened edges. (b) After joining. (c) Alignment of crystals after joining.

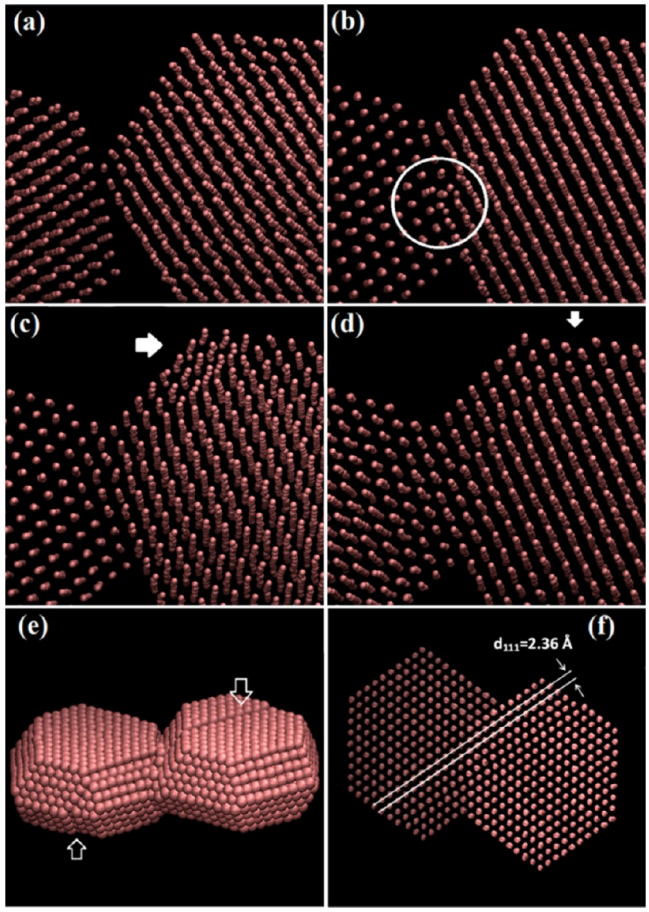

Figure 6. Hexagonal nanodisks joining at 300 K: (a) initial contact; (b) interface structure at 22 500 time steps, generated dislocation was circled; (c) movement of dislocation; (d) final interface structure; (e) the nanodisks after joining, the arrows show the plastic deformation in the particles; (f) crystal alignment of the particles after joining.

interface toward lower energy positions and other atoms followed them. During these migrations of atoms, we observed an edge dislocation that was created in the interface between the particles as shown in the circled area in Figure 6b. However, the dislocation moved out of the crystal as shown in Figure 6c. Finally, this dislocation reached the surface and made a step. These steps are pointed by arrows in Figure 6d. Final configuration of the particles is shown in Figure 6e where the plastic deformation step can be seen in both particles near the boundary, which is created through dislocation movement out from the particles. Figure 6f shows the complete alignment of the particles after joining. Note that the dislocations are created because of crystal mismatch at the interface when the particles reach each other. The same mismatch can be observed in joining of the triangular nanoparticles.

As shown in Figure 6, MD simulation revealed that nucleated dislocations at the interface are not stable and will move to the surface. Instability of dislocations in nanoparticles has been reported previously. For example, the strengthening mechanism of metals changes from Hall−Petch to inverse Hall−Petch softening at nano grain metals because of the instability of dislocation arrays in nanosize crystalline materials.[36] Not only nanocrystalline metal but also nanosize individual particles' defects are affected by the size of the crystal. Liu et al. showed that when the size of iron nanoparticles became less than a critical value, dislocation core could not be stable in the iron nanoparticles.[37] In another research, Schall et al. by using a continuum model and experimental observation showed that there is a critical radius for the particles, below which dislocations cannot be stable in the particles.[38] Jose-Yacaman et al. claimed that partial dislocations can be stable in nanoparticles,[39] and Cerlton et al. showed that stacking fault and twin defects might be stable in nanoparticles while they are rare in coarse grain material.[40] They claimed that these defects are stable in nanostructured material because of the stability of partial dislocation in nanoscale. Our modeling results are consistent with these results: hexagonal and triangular nanoparticles have stable stacking faults;[39,40] meanwhile, dislocations at the nanodisk interfaces were not stable and moved to the surface of the nanoparticles.[36,37]

To investigate the possible phase transition during joining of particles, joining of two triangular nanoparticles at higher temperatures was studied. The Lindemann indices of the particles before joining at different temperatures are reported in Figure 7a. As shown in this figure, the Lindemann index of the particle is less than 0.1 at 500 K and lower temperatures. This indicates that the joining procedure at a temperature lower than 500 K is based on a solid-state diffusion. In addition, the Lindemann indexes as a function of the distance to the center for all of the atoms of a triangular nanoparticle at 1, 300, and 500 K are presented in Figures 7b, 7c, and 7d, respectively. Figures 7b and 7c show that all atoms of the nanoparticle (surface and bulk) at 1 and 300 K are in solid state since the Lindemann index of all of the atoms are below 0.1. However, at 500 K (Figure 7d), it can be seen that a few atoms located on the vortex of the triangle have Lindemann index higher than 0.1. A high Lindemann index of these five atoms demonstrates

dx.doi.org/10.1021/jp403712x | J. Phys. Chem. C 2013, 117, 16665−16676

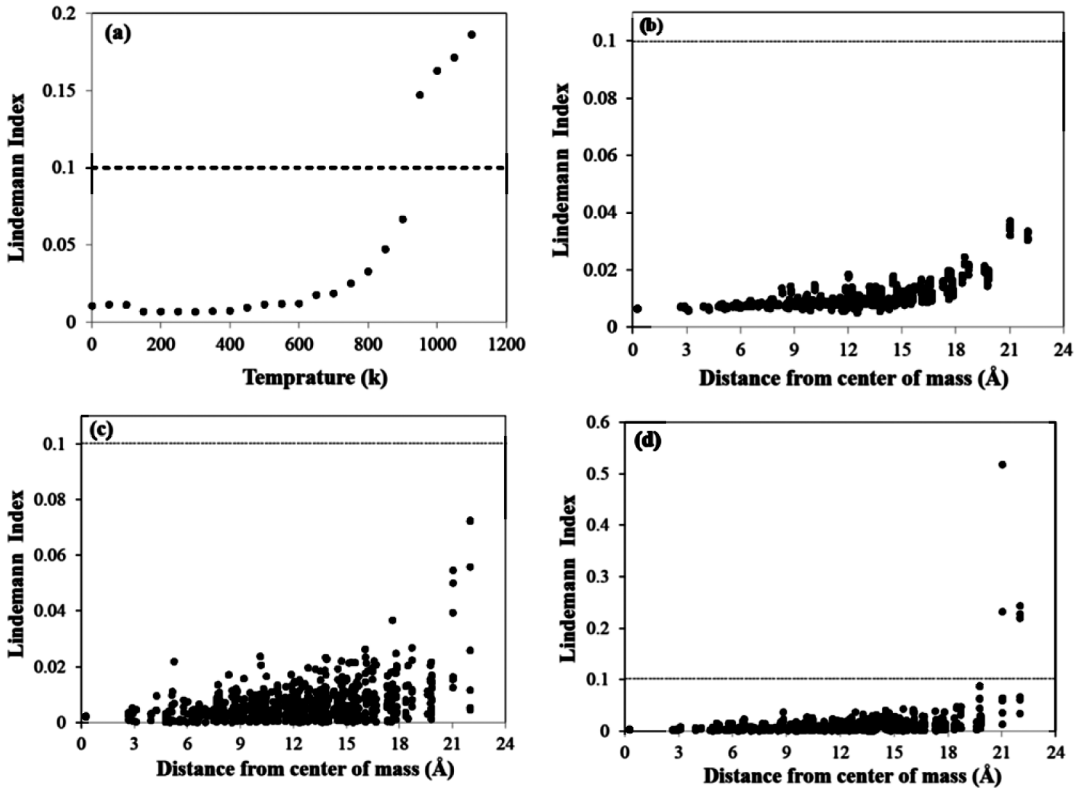

Figure 7. (a) Lindemann index of a triangular nanodisk at different temperatures. (b) Lindemann index of atoms of the triangular nanodisk at 1 K. (c) Lindemann index of atoms at 300 K. (d) Lindemann index of atoms at 500 K.

that they had higher mobility. This is an evidence for surface premelting. High mobility of these atoms seems reasonable because of the missing neighbors of the atoms at the sharp corners of triangles. Although few atoms were of high mobility, most of the atoms of the particles were in the solid state. Thus, these high mobility atoms would not affect joining of the particles too much, and it is reasonable to state that the joining was done in solid state. However, it is expected that with increasing temperatures the number of the high mobility atoms will reach a critical value and trigger a local phase transition. If that occurs, the joining will be the combined effect of both solid state diffusion and liquid phase sintering. A further detailed study at a higher temperature is under way.

Figures 8a–d show different views of the final configuration of the particles after 200 000 time steps. Our modeling reveals that the joining procedure at 500 K was the same as 1 K and 300 K, but the shapes of the initial structural blocks (triangular nanodisks) were changed during joining. The atoms at 500 K had high mobility because of increasing kinetic energy of the system by increasing temperature. In other words, silver is very soft at higher temperature, and induced energy in the system during joining can deform particles. Therefore, the interface of the nanodisks extended, and consequently, the strength of the joint is higher than other joining at lower temperature. The strength of the joints between nanoparticles is important in some applications, and high temperature solid state joining can be applicable in this kind of application although the shapes of the structural blocks have changed.

To compare the joining process at different temperatures, potential energy changes of the system during simulation at different temperatures are presented in Figure 9. As it was explained, potential energy of the system has decreased due to

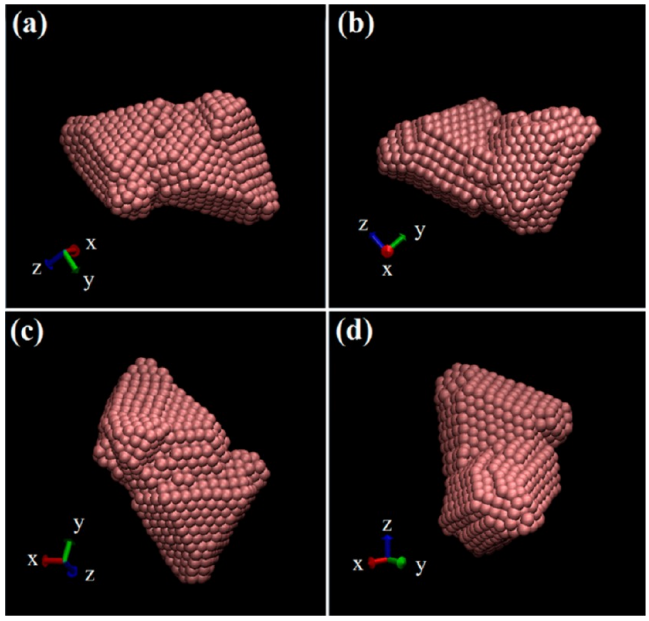

Figure 8. Final configuration of the silver triangular nanodisks after joining at 500 K from different views; the coordinate axes on each image show viewing direction.

joining. The noisy nature of the curves at 300 and 500 K is related to kinetic energy of the system. When temperature increased, the atoms vibrate, and during vibration the distances between the atoms change randomly; this leads to some noises that superimpose on the potential energy of the system. As shown in Figure 9a, the joining process at 300 K takes more time to become stable. In comparison to 1 K, joining of the

dx.doi.org/10.1021/jp403712x | J. Phys. Chem. C 2013, 117, 16665–16676

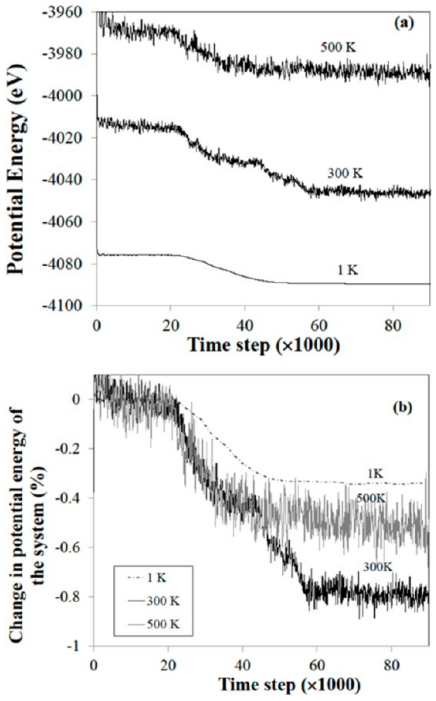

Figure 9. (a) Potential energy change of the system during joining at 1, 300, and 500 K. (b) Normalized potential energy change at 1, 300, and 500 K versus simulation time.

particles at 300 K is more complicated and leads to larger area in the boundary between the particles and hence takes more time to complete. This fact can be easily understood when comparing Figures 1c and 1d and Figures 3f and 4. On the other hand, joining at 500 K is faster than 300 K because of the higher thermal energy of the system that helps the atoms to move faster and even diffuse on the surface or in the bulk. To compare the change in energy of the system through joining at different temperatures, the changes in potential energy of the system at different temperatures with respect to the initial potential energy of the systems before joining at the same temperature are plotted in Figure 9b. This figure reveals that the potential energy drop during joining at 300 K is more than those at two other temperatures. In comparison to the 1 K, the energy reduction of the system through joining at 300 K is higher because of the larger joint area compared to the line contact joint at 1 K (Figures 1c, 3f, and 4). At 500 K, the particles deformed during joining as shown in Figure 8. These deformations create new surfaces. In contrast, joining at room temperature shows perfect alignment of the atoms. Hence, the total energy drop in 500 K is less than 300 K when the crystals did not align well at 500 K.

Both triangular and hexagonal nanoparticles are synthesized in an experiment. Therefore, their joining is predictable and should consider for simulation as a real case. Figure 10 shows MD modeling result of joining between a hexagonal and a triangular silver nanoparticle. The edges of two particles were parallel at the beginning of joining as it can be seen in Figure

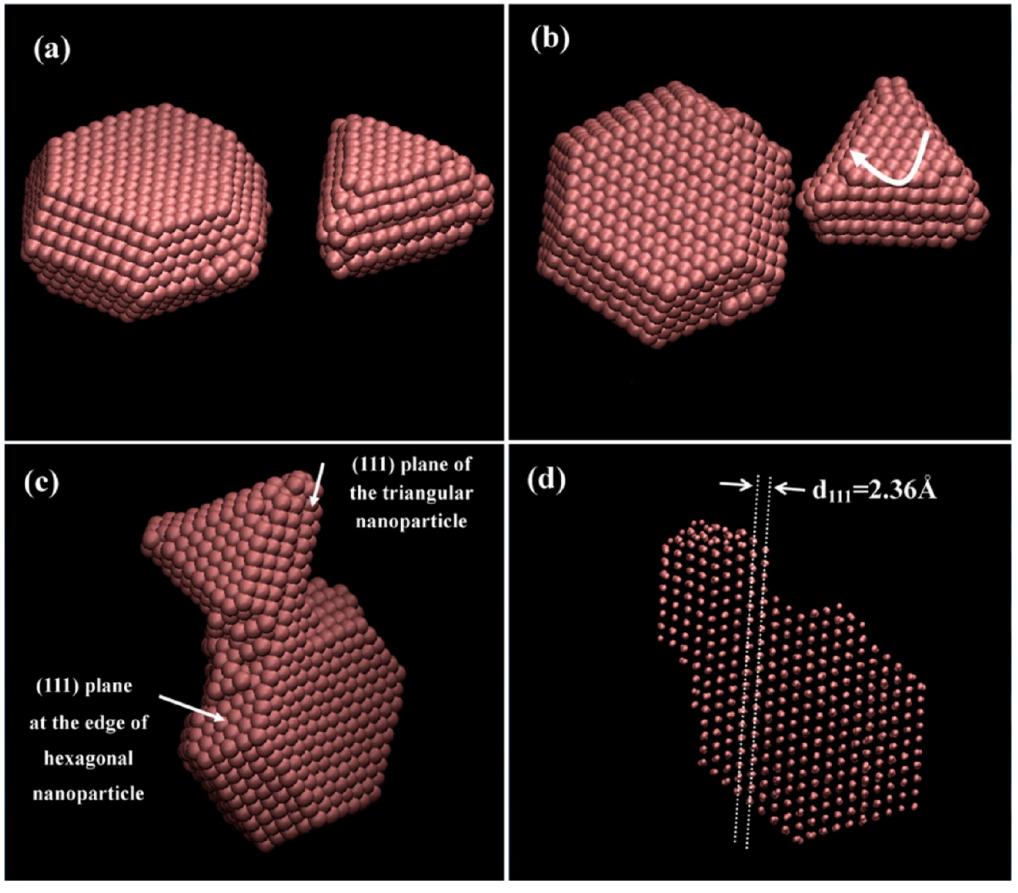

Figure 10. Joining of hexagonal and triangular nanoparticle: (a) initial configuration of the nanoparticles at the start of joining; (b) rotation of the particles before joining; (c) corner to corner join and alignment of the nanoparticles; (d) crystal structure of nanoparticles after joining.

dx.doi.org/10.1021/jp403712x | J. Phys. Chem. C 2013, 117, 16665−16676

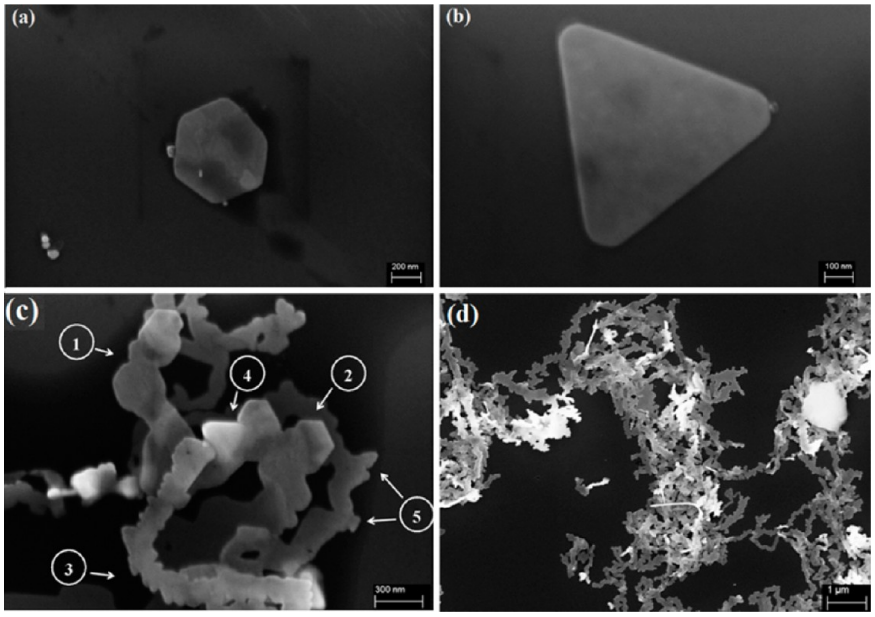

Figure 11. (a) SEM images of a hexagonal silver nanodisk. (b) SEM Images of a triangular silver nanodisk. (c) SEM image of silver nanobelts formed by joining of structural blocks. (d) Low-magnification SEM image of the nanobelts.

10a. However, it is clearly shown in Figure 10b that the particles rotated while they migrate toward each other. The arrow in Figure 10b shows the rotation direction of the triangular nanoparticle. Figure 10c shows the nanoparticles after joining. As it can be seen in this figure, the particles rotated and joined in a corner−corner configuration. Figure 10c shows that the (111) plane of the triangular particles is aligned with the (111) plane at the edge of hexagonal nanoparticle which is compatible with other joining of triangular particles and hexagonal particles that are shown in Figures 6f and 4. Figure 10f unveiled the perfect crystal alignment between the joined hexagonal and triangular silver nanoparticles by decreasing size of the ball with visualization software. The image viewed perpendicular to the (111) plane of the hexagonal particles indicates that the triangular particle rotated and aligned with the (111) plane at the edge of hexagonal nanoparticles.

The rotation of nanoparticles during migration of the particles before joining depicted in Figure 10 shows the importance of nanoparticle's geometry and its impact on the self-assembly of the particles. The Lindemann index of atoms of triangular nanoparticles presented in Figure 7 shows that the atoms at the corner of the triangular particles have a higher mobility, which means a higher energy in comparison to the atoms inside or at the surface far from corners. High energy levels of the atoms at the corners of triangular particle lead to a higher tendency of these atoms to join to their neighbors to reduce their energy levels. Therefore, during the migration of hexagonal and triangular particles, the higher attraction force at the corners drives the particle to rotate and creates contacts at high-energy corners. Therefore, it can be deduced that the shape of nanoparticles and its effect on the energy of the surface atoms are the important parameters in the self-assembly of the particles. It is worthwhile to emphasize that this case is still a special configuration for joining of the hexagonal and rectangular nanoparticles. Other parameters, such as the sizes of particles, their initial velocities when they approach each other, absorbed surface molecules, and so on, can affect the self-assembly of the particles and should be taken into account.

Overall, the MD simulation shows that the silver nanodisks are able to join to each other even at 1 K by movement of the surface atoms because of atomic attraction. These movements of atoms occurred because of the high energy of surface atoms at a nanoscale.[41−44] The surface atoms of nanoparticles are excited, and their bond with other atoms is weaker than surface atoms of micrometer size particles, which means their energy is higher than surface atoms of micrometer size particles.[42] Therefore, when two nanoparticles become enough close and their surface atoms attract each other, this attraction force can be enough strength to pull out them from their position on the surface and guide to a new position. Hence, the atoms make a new bond and reduce their energy. This energy release is the driving force for movement of atoms and joining. On the other hand, continuity of the crystals in solid state leads to rearrangement of the neighbors of the migrated atoms. These fast migrations of atoms store elastic energy in the system through elongation of the atomic bonds around the jumped atoms. This excess energy will be released through elastic or plastic deformation. The joining process is fast and finished within few thousand time steps. Hence, the joining mechanism at room temperature is different from diffusional process, which is the dominant mechanism of sintering at high temperature (above half of melting point of the material). Another important outcome of the simulation is alignment of the crystals after joining at room temperature (300 K). In comparison to 1 K, joining of the particles at 300 K has more progress after first atom contact. The mechanism of the first attachment of the particles at 300 K is similar to that at 1 K. However, at 300 K the atoms have more kinetic energy than at 1 K, which means the atoms have more vibration. Therefore, the surface atoms of the particles in the joining area have more chance to move toward each other. Hence, the joining process can show more progress in comparison to joining at 1 K. Based on our findings, the interface of joined nanodisks at 300 K will be free from crystal defects, and the joining at room

temperature serves as the lowest energy condition to the particles in comparison to joining at very higher and lower temperature. As mentioned earlier, room temperature joining and crystal alignment were reported by other researchers.[8,9,11,12,14,45] They reported that nanoparticles could assemble and join at room temperature and after joining. In some cases, crystal alignment was also observed. These experimental observations emphasize that the results of our MD simulation are reliable. Therefore, the provided mechanism for low-temperature nanojoining can be used to explain how and why nanoparticles join to each other in different conditions. Another important feature observed in our MD modeling is the existence of different interface conditions between the particles at different temperatures. At 1 K, the interface is restricted to line contact. This type of interface can be employed in some applications such as sensing because of localized surface plasmonic hot spots.[44] At 300 K, the interface of the joined nanodisk is more extended. This area will be a perfect crystal without usual defects such as dislocations. In this condition, the particles are joined and aligned; meanwhile, their initial shapes remain intact. These interesting features of the nanojoining at 300 K introduce unique and novel morphology for silver in nanoscale. From this point of view, 500 K is too hot to keep the initial shape of the particles intact. The particles will deform at high temperature solid state joining, and the bond between the particles will be strong.

We did some experiments to validate our MD simulation results. To do that, we employed a wet chemical route to synthesize, self-assemble, and join hexagonal and triangular silver nanoparticles. Synthesized silver nanoparticles structural blocks are shown in Figures 11a and 11b individually. It is worthwhile to emphasize that the hexagonal and triangular structural blocks were almost joined to each other. Only few individual structural blocks can be observed in the product. Crystal structures of the silver hexagonal and triangular nanodisks that were synthesized in the experimental part of this research are well-known.[33,35,46,47] In these two kinds of nanodisks, each crystal consists of a twin plane in the middle of the particle. Since the stacking fault energy of silver is quite low, the twin plane can be formed easily. Therefore, the top and bottom planes of the crystal will be (111). The edges of the crystal consisted of (111) and (100) planes. The initial crystal shape will be hexagonal because of the symmetry of fcc structure. These hexagonal nanoparticles will grow to make a triangular shape crystal because of different growth rates in [111] and [100] directions. To synthesize silver structural blocks, we used ascorbic acid as the reducing agent[33,48] and PMAA as stabilizing/capping agent. PMAA was used as reducing agent to reduce Ag^+ to Ag by itself; however, as reported by Zhang et al., this process is very slow and needs long aging time.[49] Since our synthesis was very fast and finished in few minutes, it indicates that PMAA cannot function as a dominant reducing agent by attaching to Ag ions, although some silver ions can attach to PMAA. On the other hand, PMAA molecules could attach to the Ag crystals after reduction.[50] The surface atoms of silver particles desired to share their energy and become more stable. Therefore, PMAA molecules may attach to the surface atoms of the small silver particles. On the basis of published papers and also the shape of the synthesized silver nanoparticles presented in Figures 11a and 11b, it can be assumed that the PMAA molecules were attached to the (111) planes of initial silver clusters. The PMAA that covered the top and bottom sides of the particles reduced the chance of joining of the particles from the big flat sides; however, they could touch from the edges and join. This is compatible with our edge-to-edge and edge-to-corner MD simulation so we could compare the experimental and MD results.

SEM images of self-assembled and joined silver nanoparticles are shown in Figure 11c. The hexagonal and triangular silver particles were attached to each other and result in nanobelts. Different joining configurations can be seen in Figure 11c. The marks of "one" and "two" in the figure indicate the positions where hexagonal structural blocks joined to each other. The area marked by "three" shows the triangular structural blocks join together. The head to the corner or edge configuration of these triangular nanoparticles is compatible with MD simulation results presented in Figure 10. The mark of "four" points to the joining of hexagonal and triangular blocks while these blocks keep their initial shapes. Two triangular nanoparticles marked by "five" in Figure 11c have been joined in two different configurations to a nanobelt, indicating a random nature of the self-assembly of the structural blocks. Figure 11d shows a low-magnification SEM image of nanobelts consisting of the silver structural blocks. This image reveals that the structure and joining configuration shown in Figure 11c are uniformly distributed through the whole sample. These two SEM images prove that the nanoparticles can join to each other at room temperature. This is consistent with our MD simulation results (Figures 3−6 and 10). To check the important alignment feature of the nanojoining at room temperature that was revealed by the MD simulation, we performed HRTEM observation. Figures 12a and 12b show a

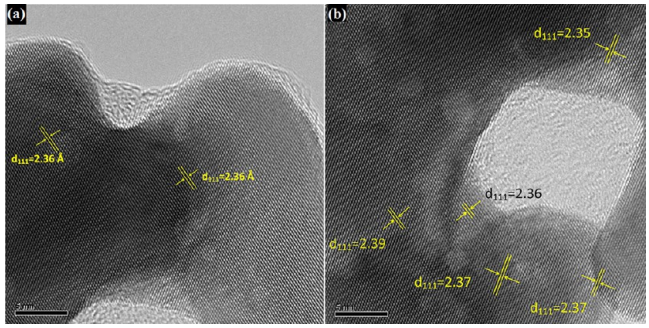

Figure 12. (a) HRTEM image of the interface area between two joined nanodisks; direction of (111) planes of the particles are marked. (b) HRTEM image of five silver nanodisks after joining; directions of (111) planes of the particles are marked.

HRTEM image of the boundary area between the nanoparticles. Figure 12a reveals two nanoparticles that joined to each other and perfectly aligned. As shown in Figure 12a, the particles were joined and aligned on their (111) planes. The crystal structure of the boundary between two particles was perfect as predicted through MD simulation (Figure 6f). More evidence of the joint morphology is presented in Figure 12b. In this image, five particles were joined to each other, and as clearly shown, all of the particles tended to achieve their lowest energy level by aligning their crystal structure, which was predicted by our MD simulation in Figures 4, 6d, and 6f. (111) planes of five particles are marked in Figure 12b. The experimental outcomes have supported our MD simulation results and show that nanojoining can be considered as a synthesis method to build nanostructures. In addition, the

boundaries of the joined particles had perfect crystal structure as predicted by the MD simulations.

CONCLUSION

In this research, we have employed molecular dynamics simulation method to study room temperature joining of silver nanoparticles as an applicable noble material. Our MD simulation has shown that low-temperature joining occurred by short movement of atoms to reach lower energy levels. These atoms have forced their adjacent atoms to follow them and impose elastic strain on the crystal structure, which are released through subsequent elastic deformation of the particles. If crystal defects such as dislocations are created in the interface during joining, they will move out and make plastic deformation in the particles, and after these events, the final crystal structure of the particles will align and reach minimum energy level. This decrease in the energy of the surface atoms is the driving force for nanoparticle joining at room temperature. Our MD simulations at lower temperature show that the joining can occur even at 1 K. However, energy of the system is not sufficient to make a complete joint between the particles. At this temperature, the particles assembled and made a line contact. The mechanism of joining at 1 K is short movement of atoms from their position on the surface of a particle toward surface atoms of the other particle followed by subsequent elastic deformation to release stored elastic energy. In contrast, at 300 K, the particles not only make a line-contact joint at beginning but also the joint grows to cover the whole interface area between two nanoparticles. In this condition, the original shapes of the structural blocks will remain intact. This phenomenon is very important for assembled nanoparticles to fabricate nanodevices. At higher temperature (500 K), the particles are very ductile, stored energy during migration of atoms is enough to do plastic deformation, and shapes of the structural blocks will change. Therefore, the final product is more like sintering of the nanoparticles. Experimentally, synthesized silver hexagonal and triangular nanodisks were self-assembled and joined into nanobelt morphology simultaneously, which is compatible with our MD simulation results. In addition, HRTEM clarified that the interface area of the joined particles is perfect, and no dislocations remain in the interface. This observation confirms our MD simulation results that show generated dislocations will move out, and the final crystal structure of the joined particles will be perfect.

AUTHOR INFORMATION

Corresponding Author

*E-mail: a2hu@mecheng1.uwaterloo.ca (A.H.).

Notes

The authors declare no competing financial interest.

ACKNOWLEDGMENTS

This work was supported by the strategic research funds from the Natural Sciences and Engineering Research Council of Canada (NSERC).

REFERENCES

(1) Zhou, Y.; Hu, A.; Khan, M. I.; Wu, W.; Tam, B.; Yavuz, M. Recent Progress in Micro and Nano-joining. *J. Phys.: Conf. Ser.* **2009**, *165*, 012012 (1−6).

(2) Israelachvili, J. N. *Intermolecular and Surface Forces*, 3rd ed.; Academic Press: San Diego, 2011.

(3) Kittel, C. *Introduction to Solid State Physics*; John & Sons Inc.: New York, 1996.

(4) Fang, Z. Z.; Wang, H. Densification and Grain Growth during Sintering of Nanosized Particles. *Int. Mater. Rev.* **2008**, *53*, 326−352.

(5) Seiz, F.; Turnbull, D. *Solid State Physics*; Academic Press: New York, 1964; Vol. *16*.

(6) Frankel, D.; Smit, B. *Understanding Molecular Simulation: From Algorithms to Applications*; Academic Press: San Diego, 1996.

(7) Murphy, C. J.; Sau, T. K.; Gole, A. M.; Orendorff, C. J.; Gao, J.; Gou, L.; Hunyadi, S. E.; Li, T. Anisotropic Metal Nanoparticles: Synthesis, Assembly, and Optical Applications. *J. Phys. Chem. B* **2005**, *109*, 13857−13870.

(8) Li, M.; Schnablegger, H.; Mann, S. Coupled Synthesis and Self-assembly of Nanoparticles to Give Structures with Controlled Organization. *Nature* **1999**, *402*, 393−395.

(9) Gao, Y.; Jiang, P.; Liu, D. F.; Yuan, H. J.; Yan, X. Q.; Zhou, Z. P.; Wang, J. X.; Song, L.; Liu, L. F.; Zhou, W. Y.; Wang, G.; Wang, C. Y.; Xie, S. S. Synthesis, Characterization and Self-assembly of Silver Nanowires. *Chem. Phys. Lett.* **2003**, *380*, 146−149.

(10) Grzelczak, M.; Vermant, J.; Furst, E. M.; Liz-Marzan, L. M. Directed Self-Assembly of Nanoparticles. *ACS Nano* **2010**, *4*, 3591−3605.

(11) Sun, Y.; Mayers, B.; Xia, Y. Transformation of Silver Nanospheres into Nanobelts and Triangular Nanoplates through a Thermal Process. *Nano Lett.* **2003**, *3*, 675−679.

(12) Tang, Z.; Kotov, N. A.; Giersig, M. Spontaneous Organization of Single CdTe Nanoparticles into Luminescent Nanowires. *science* **2002**, *297*, 237−240.

(13) Gates, B.; Wu, Y.; Yin, Y.; Yang, P.; Xia, Y. Single-Crystalline Nanowires of Ag_2Se Can Be Synthesized by Templating against Nanowires of Trigonal. *J. Am. Chem. Soc.* **2001**, *123*, 11500−11501.

(14) Korgel, B. A.; Fitzmaurice, D. Self-Assembly of Silver Nanocrystals into Two-Dimensional Nanowire Arrays. *Adv. Mater.* **1998**, *10*, 661−665.

(15) Kalsin, A. M.; Fialkowski, M.; Paszewski, M.; Smoukov, S. K.; Bishop, K. J. M.; Grzybowski, B. A. Electrostatic Self-Assembly of Binary Nanoparticle Crystals with a Diamond-Like Lattice. *Science* **2006**, *312*, 420−424.

(16) Zhang, X.-Y.; Hu, A.; Zhang, T.; Lei, W.; Xue, X.-J.; Zhou, Y.; Duley, W. W. Self-Assembly of Large-Scale and Ultrathin Silver Nanoplate Films with Tunable Plasmon Resonance Properties. *ACS Nano* **2011**, *5*, 9082−9092.

(17) Chacko, S.; Joshi, K.; Kanhere, D. G. Why Do Gallium Clusters Have a Higher Melting Point Than the Bulk? *Phys. Rev. Lett.* **2004**, *13*, 135506 (1−4).

(18) Lehtinen, K. E. J.; Zachariah, M. R. Effect of Coalescence Energy Release on the Temporal Shape Evolution of Nanoparticles. *Phys. Rev. B* **2001**, *63*, 205402 (1−7).

(19) Ding, F.; Rosén, A.; Bolton, K. Size Dependence of the Coalescence and Melting of Iron Clusters: A Molecular-Dynamics Study. *Phys. Rev. B* **2004**, *70*, 075416 (1−6).

(20) Ding, F.; Bolton, K.; Rośen, A. Molecular Dynamics Study of the Surface Melting of Iron Clusters. *Eur. Phys. J. D* **2005**, *34*, 275−277.

(21) Arcidiacono, S.; Bieri, N. R.; Poulikakos, D.; Grigoropoulos, C. P. On the Coalescence of Gold Nanoparticles. *Int. J. Multiphase Flow* **2004**, *30*, 979−994.

(22) Shvartsburg, A. A.; Jarrold, M. F. Solid Clusters above the Bulk Melting Point. *Phys. Rev. Lett.* **2000**, *12*, 2530−2532.

(23) Hu, A.; Guo, J. Y.; Alarifi, H.; Patane, G.; Zhou, Y.; Compagnini, G.; Xu, C. X. Low Temperature Sintering of Ag Nanoparticles for Flexible Electronics Packaging. *Appl. Phys. Lett.* **2010**, *97*, 153117 (1−3).

(24) Guo, J. Y.; Xu, C. X.; Hu, A. M.; Oakes, K. D.; Sheng, F. Y.; Shi, Z. L.; Dai, J.; Jin, Z. L. Sintering Dynamics and Thermal Stability of Novel Configurations of Ag Clusters. *J. Phys. Chem. Solids* **2012**, *73*, 1350−1357.

(25) Qi, W. H.; Wang, M. P. Size Effect on the Cohesive Energy of Nanoparticle. *J. Mater. Sci. Lett.* **2002**, *21*, 1743−1745.

(26) Humphrey, W.; Dalke, A.; Schulten, K. VMD- Visual Molecular Dynamic. *J. Mol. Graphics* **1996**, *14*, 33−38.
(27) Daw, M. S.; Baskes, M. I. Semiempirical, Quantum Mechanical Calculation of Hydrogen Embrittlement in Metals. *Phys. Rev. Lett.* **1983**, *50*, 1285−1288.
(28) Daw, M. S.; Baskes, M. I. Embedded-Atom Method: Derivation and Application to Impurities, Surfaces, and Other Defects in Metals. *Phys. Rev. B* **1984**, *29*, 6443−6453.
(29) Foiles, S. M.; Baskes, M. I.; Daw, M. S. Embedded-Atom-Method Functions for fcc Metals Cu, Ag, Au, Ni, Pd, Pt, and Their Alloys. *Phys. Rev. B* **1986**, *33*, 7983−7991.
(30) Hoover, W. G. Canonical Dynamics: Equilibrium Phase-Space Distributions. *Phys. Rev. A: At. Mol. Opt. Phys.* **1985**, *31*, 1695−1697.
(31) Hail, J. M. *Molecular Dynamics Simulation: Elementary Methods*; John Wiley & Sons: New York, 1992.
(32) Ding, F.; Bolton, K.; Rosen, A. Molecular Dynamics Study of the Surface Melting of Iron Clusters. *Eur. Phys. J. D* **2005**, *34*, 275−277.
(33) Aherne, D.; Ledwith, D. M.; Gara, M.; Kelly, J. M. Optical Properties and Growth Aspects of Silver Nanoprisms Produced by a Highly Reproducible and Rapid Synthesis at Room Temperature. *Adv. Funct. Mater.* **2008**, *18*, 2005−2016.
(34) Qi, W. H.; Lee, S. T. Core−Shell Structures of Silicon Nanoparticles and Nanowires with Free and Hydrogenated Surface. *Chem. Phys. Lett.* **2009**, *483*, 247−249.
(35) Elechiguerra, J. L.; Reyes-Gasga, J.; Yacaman, M. J. The Role of Twinning in Shape Evolution of Anisotropic Noble Metal Nanostructures. *J. Mater. Chem.* **2006**, *16*, 3906−3919.
(36) Song, H. W.; Guo, S. R.; Hu, Z. Q. A Coherent Polycrystal Model For The Inverse Hall-Petch Relation in Nanocrystalline Materials. *Nanostruct. Mater.* **1999**, *11*, 203−210.
(37) Liu, H. B.; Canizal, G.; Jimenez, S.; Espinosa-Medina, M. A.; Ascencio, J. A. Molecular Dynamics Simulation on Edge Dislocation in the Bulk and Nanoparticles of Iron. *Comput. Mater. Sci.* **2003**, *27*, 333−341.
(38) Schall, P.; Cohen, I.; Weitz, D. A.; Spaepen, F. Visualizing Dislocation Nucleation by Indenting Colloidal Crystals. *Nature* **2006**, *440*, 319−323.
(39) Jose-Yacaman, M.; Perez-Tijerinab, E.; Mejia-Rosales, S. Defect Structure in Nanoalloys. *J. Mater. Chem.* **2007**, *17*, 1035−1038.
(40) Carlton, C. E.; Rabenberg, L.; Ferreira, P. J. On the Nucleation of Partial Dislocations in Nanoparticles. *Philos. Mag. Lett.* **2008**, *88*, 715−724.
(41) Chamaani, A.; Marzbanrad, E.; Rahimipour, M. R.; Yaghmaee, M. S.; Aghaei, A.; Kamachali, R. D.; Behnamian, Y. J. Thermodynamics and Molecular Dynamics Investigation of a Possible New Critical Size for Surface and Inner Cohesive Energy of Al Nanoparticles. *Nanopart. Res.* **2011**, *13*, 6059−6067.
(42) Qi, W.; Huang, B.; Wang, M. Bond-Length and -Energy Variation of Small Gold Nanoparticles. *J. Comput. Theor. Nanosci.* **2009**, *6*, 635−639.
(43) Qi, W. H. Modeling the Relaxed Cohesive Energy of Metallic Nanoclusters. *Mater. Lett.* **2006**, *60*, 1678−1681.
(44) Hu, A.; Peng, P.; Alarifi, H.; Zhang, X. Y.; Guo, J. Y.; Zhou, Y.; Duley, Y. Y. Femtosecond Laser Welding Nanostructures and Plasmonic Devices. *J. Laser Appl.* **2012**, *24*, 0420011−0420017.
(45) Peng, P.; Liu, L.; Gerlich, A. P.; Hu, A.; Zhou, Y. N. Self-Oriented Nanojoining of Silver Nanowires via Surface Selective Activation. *Part. Part. Syst. Charact.* **2013**, *5*, 420−426.
(46) Maillard, M.; Giorgio, S.; Pileni, M.-P. Silver Nanodisks. *Adv. Mater.* **2002**, *14*, 1084−1086.
(47) Yang, Y.; Matsubara, S.; Xiong, L.; Hayakawa, T.; Nogami, M. Solvothermal Synthesis of Multiple Shapes of Silver Nanoparticles and Their SERS Properties. *J. Phys. Chem. C* **2007**, *111*, 9095−9104.
(48) Songping, W.; Shuyuan, M. Preparation of Ultrafine Silver Powder Using Ascorbic Acid as Reducing Agent and Its Application in MLCI. *Mater. Chem. Phys.* **2005**, *89*, 423−427.
(49) Zhang, D.; Qi, L.; Ma, J.; Cheng, H. Formation of Silver Nanowires in Aqueous Solutions of a Double-Hydrophilic Block Copolymer. *Chem. Mater.* **2001**, *13*, 2753−2755.
(50) Ishizu, K.; Kakinuma, H.; Ochi, K.; Uchida, S.; Hayashi, M. Encapsulation of Silver Nanoparticles Within Double-Cylinder-Type Copolymer Brushes as Templates. *Polym. Adv. Technol.* **2005**, *16*, 834−839.